Journal of Medicinal Chemistry

Article

pubs.acs.org/jmc

In Vitro Anticancer Activity of *cis*-Diammineplatinum(II) Complexes with β-Diketonate Leaving Group Ligands

Justin J. Wilson and Stephen J. Lippard*

Department of Chemistry, Massachusetts Institute of Technology, Cambridge, Massachusetts 02139, United States

Supporting Information

ABSTRACT: Five cationic platinum(II) complexes of general formula, $[Pt(NH_3)_2(\beta\text{-diketonate})]X$ are reported, where X is a noncoordinating anion and β-diketonate = acetylacetonate (acac), 1,1,1,-trifluoroacetylacetonate (tfac), benzoylacetonate (bzac), 4,4,4-trifluorobenzoylacetonate (tfbz), or dibenzoylmethide (dbm), corresponding, respectively, to complexes **1**–**5**. The log *P* values and the stabilities of **1**–**5** in aqueous solution were evaluated. The phenyl ring substituents of **3**–**5** increase the lipophilicity of the resulting complexes, whereas the trifluoromethyl groups of **2** and **4** decrease the stability of the complexes in aqueous solution. The uptake of **1**–**5** in HeLa cells increases as the lipophilicity of the investigated complex increases. Cancer cell cytotoxicity studies indicate that **1** and **3** are the least active complexes whereas **2**, **4**, and **5** are comparable in activity to cisplatin.

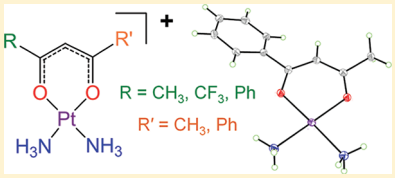

INTRODUCTION

Cisplatin is an effective anticancer drug in clinical use worldwide.[1] The amelioration of toxic side effects associated with the use of this drug was an impetus for the development of the second-generation platinum chemotherapeutic agent, carboplatin (Chart 1).[2,3] Cisplatin and carboplatin operate by the same mechanism. Labile ligands in the coordination sphere, chloride for cisplatin and 1,1-cyclobutanedicarboxylate (CBDCA) for carboplatin, are displaced by water or other biological nucleophiles, and the activated *cis*-diammineplatinum(II) moiety binds to purine bases in nuclear DNA.[4] The resulting platinum-DNA adducts, chiefly 1,2-intrastrand cross-links, ultimately kill the cancer cell through transcription inhibition and subsequent downstream effects.[5] Because cisplatin and carboplatin bear the same NH_3 nonleaving group ligands, the resulting DNA adducts are identical,[6] and therefore, the drugs exhibit the same spectrum of activity.[7] Carboplatin, however, is significantly less toxic than cisplatin. The typical patient dose for carboplatin is approximately ten times greater than that of cisplatin (400 mg/m^2 versus 40 mg/m^2), and the dose-limiting toxic side effect of carboplatin is myelosuppression in contrast to nephrotoxicity for cisplatin.[8] These important clinical differences reveal that the leaving group ligands play an integral role in modulating toxic side effects. Further modification of these units may therefore be of value in the search for new platinum anticancer drug candidates.

As anticipated, the properties of carboplatin spurred the design of cisplatin analogues having other leaving groups.[9−22] The departing ligands of platinum anticancer agents influence not only the aquation rate but also the lipophilicity of the resulting complex. Both parameters, as exemplified by carboplatin, influence overall pharmacokinetic properties. Leaving group modifications have been applied to a class of cytotoxic platinum(II) complexes in which the remaining ligands have trans stereochemistry, an interesting development in view of the fact that the trans isomer of cisplatin is inactive.[23] Exchange of the original halide leaving groups of these trans

Chart 1

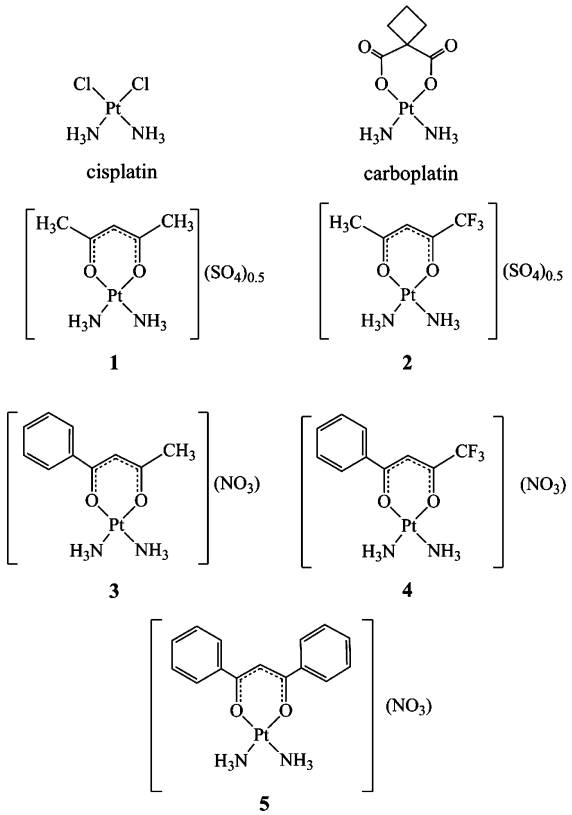

Received: February 28, 2012
Published: May 18, 2012

Scheme 1

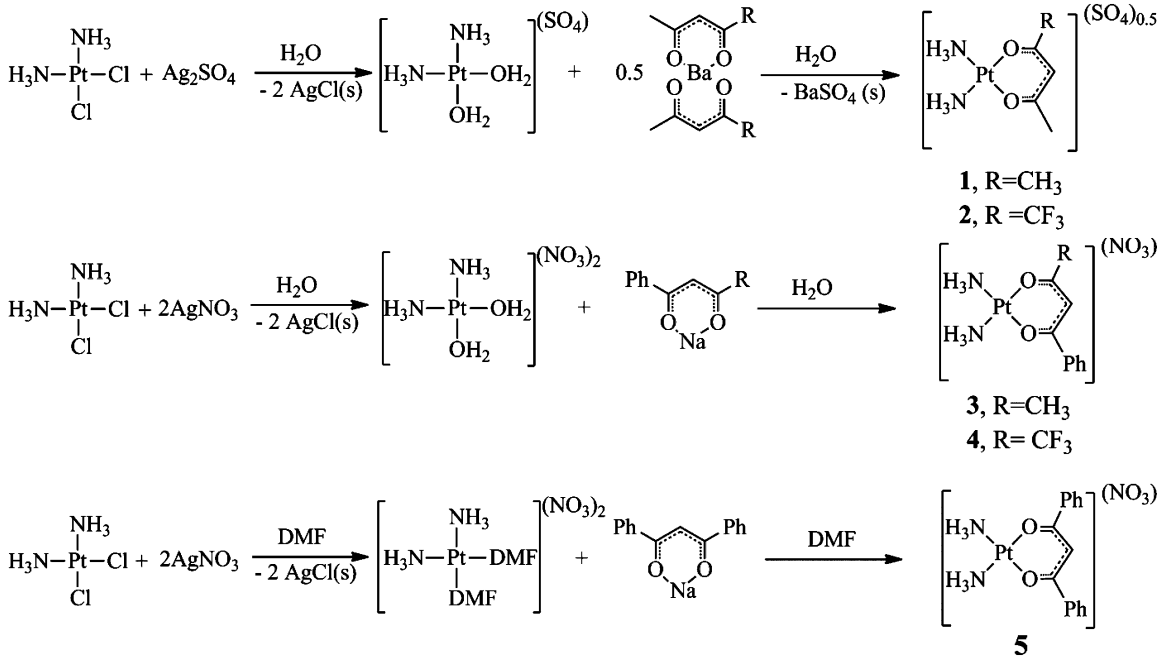

platinum(II) compounds with carboxylates led to new complexes with improved aqueous solubility, hydrolytic stability, and cellular uptake.[24−28]

Acetylacetonate (acac) and related β-diketonates form a diverse class of ligands with many applications in inorganic chemistry. The primary *O*,*O*′ bidentate chelating mode of these ligands is analogous to that of the CBDCA ligand of carboplatin, thus warranting consideration of their use as leaving group ligands for novel platinum anticancer drug candidates. Although β-diketonates have been used as supporting ligands for titanium(IV)[29,30] and organometallic ruthenium(II) anticancer agents,[31−34] few studies describe their potential utility in platinum-based therapeutic agents. In an early investigation, the complex [Pt(1,2-diaminocyclohexane)(acac)](NO_3) was synthesized, but it displayed poor antitumor activity in vivo.[35] On the basis of the structure−activity relationships at the time,[36] the authors attributed this poor activity to the positive charge of the complex. More recently, the complex, [Pt(*O*,*O*′-acac)(γ-acac)(dimethylsulfide)], was investigated for its anticancer properties.[37−40] This nonconventional anticancer platinum complex apparently exerts its biological properties through a mechanism other than DNA binding. Only the γ-coordinated acac ligand behaves as a leaving group.

Here, we report the results of our investigations of platinum anticancer drug candidates in which β-diketonate ligands serve as leaving groups. Five *cis*-diammineplatinum(II) complexes bearing different β-diketonates were prepared and characterized (Chart 1). The particular ligands were selected to systematically modify the electronic properties and hydrophobicity of the resulting platinum complexes through the use of trifluoromethyl and phenyl groups, respectively. We discovered that both of these properties have a direct effect on the overall cytotoxicity of the resulting complexes in cancer cells.

RESULTS

Synthesis and Characterization. We synthesized the platinum β-diketonate complexes by three different routes using cisplatin as a common starting material (Scheme 1). In all three approaches, cisplatin was first activated by treatment with the appropriate Ag(I) salt to remove the chloride ligands as insoluble AgCl and generate reactive solvated *cis*-diammineplatinum(II) cations. Subsequent treatment with the appropriate salt of the β-diketonate ligand afforded **1**−**5** (Scheme 1). The disparate solubilities of the β-diketonate ligands and the final platinum(II) complexes necessitated the use of the three slightly different routes shown in Scheme 1, as will be described in more detail subsequently.

Characterization of the complexes was achieved by NMR and IR spectroscopy, electrospray ionization mass spectrometry (ESI-MS), and elemental analysis. The presence of nitrate as the counterion for **3**−**5** was verified both by the characteristic N−O stretching band in the IR spectrum near 1383 cm^{-1} and by an ESI-MS *m*/*z* peak corresponding to the nitrate adduct, $[2\ M + NO_3]^+$. In the mass spectra of **1** and **2**, only the molecular ion arising from the cationic platinum complex was observed. The IR spectra of **1**−**5** are consistent with *O*,*O*′-coordination of the β-diketonate ligands. Vibrational frequencies between 1560 and 1590 cm^{-1} correspond to C═O stretches[41] and indicate a decrease in C═O bond order, consistent with π electron delocalization through the six-membered chelate ring. Elemental analyses are in agreement with the anticipated molecular formulas.

The complexes were also studied by multinuclear NMR spectroscopy (Figures S1−S16, Supporting Information). The low solubility of **2** in aqueous and organic solvents precluded acquisition of its ^{13}C NMR spectrum. For the other complexes, all expected resonances were observed in the ^{13}C NMR spectra. The trifluoromethyl groups of **2** and **4** appear at −76.43 and −76.17 ppm, respectively, in the ^{19}F NMR spectra. The ^{1}H NMR spectra display the expected resonances except for the protons of the coordinated NH_3 ligands, which are not observed, presumably due to rapid exchange with deuterons of the methanol-d_4 NMR solvent. Protons at the gamma position of the β-diketonate ligands resonate between 5.58−6.94 ppm in the five complexes, as summarized in Table 1. The

dx.doi.org/10.1021/jm3002857 | J. Med. Chem. 2012, 55, 5326−5336

^{195}Pt NMR spectra of the complexes are marked by a single peak that ranges from −1593 to −1454 ppm depending on the β-diketonate ligand (Table 1).

Table 1. Selected ^{1}H, ^{13}C, ^{19}F, and ^{195}Pt NMR Chemical Shifts (ppm) for 1−5

compd	δ ^{1}H, γ position[a]	δ ^{13}C, γ position[a]	δ ^{195}Pt[b]	δ ^{19}F[c]
1	5.58	103.3	−1593	
2	6.10	n.d.[d]	−1497	−76.43
3	6.32	100.3	−1572	
4	6.72	96.5	−1454	−76.17
5	6.96	97.5	−1528	

[a]Referenced to $SiMe_4$ at δ = 0 ppm. [b]Referenced to Na_2PtCl_6 at δ = 0 ppm. [c]Referenced to $CFCl_3$ at δ = 0 ppm. [d]Not determined.

Single crystals of **3** and **4** were obtained by vapor diffusion of diethyl ether into methanol solutions of the compounds, enabling their structures to be determined by X-ray crystallography. The results are presented in Figure 1, with relevant bond lengths and angles reported in Table 2. The structures confirm the expected square planar coordination geometries of the platinum(II) center and the *O*,*O*′-coordination mode of the β-diketonate ligands. The nitrate counterions are engaged in hydrogen bonding interactions with the protons of the coordinated NH_3 ligands (not shown).

Lipophilicity. To quantify the lipophilicity of the new platinum complexes, water−octanol partition coefficients (*P*) were measured using the shake-flask method. The resulting log *P* values are reported in Table 3 and graphically compared in Figure 2. The measured log *P* of cisplatin is consistent with literature values.[42] The most lipophilic complex is **5**, with a log *P* value of 0.0 ± 0.1. The overall order of lipophilicity follows the sequence **5** > **4** > **3** > **2** > **1**. The phenyl groups in **3**, **4**, and **5** have a larger effect on the lipophilicity than the trifluoromethyl groups of **2** and **4**. Substitution of a phenyl for a methyl group on the β-diketonate ligand leads to an increase of lipophilicity by approximately 1 log *P* unit, whereas the analogous substitution for a trifluoromethyl group leads to an increase of approximately 0.3 log *P* units.

The log *P* values of the free β-diketonate ligands in the keto form were calculated using the online program ALOGSP 2.1[43] available at the Virtual Computational Chemistry Laboratory.[44,45]

Table 2. Selected Interatomic Distances (Å) and Angles (Deg) for 3 and 4[a]

	3	4
Pt1−N1	2.034(2)	2.017(3)
Pt1−N2	2.030(2)	2.015(2)
Pt1−O1	1.9956(17)	2.005(2)
Pt1−O2	1.9907(18)	1.988(2)
O1−Pt1−O2	95.20(7)	94.69(9)
O1−Pt1−N1	86.81(8)	88.69(10)
O1−Pt1−N2	177.62(9)	176.19(10)
O2−Pt1−N1	177.79(8)	176.54(10)
O2−Pt1−N2	85.37(8)	86.12(10)
N1−Pt1−N2	92.65(9)	90.55(11)

[a]Atoms are labeled as shown in Figure 1. Numbers in parentheses are estimated standard deviations of the last significant figures.

Table 3. Experimentally Measured Complex and Computed Ligand log *P* Values

compd	measured complex log *P*[a]	calculated ligand log *P*[b]
1	−2.67 ± 0.08	0.09 ± 0.35
2	−2.28 ± 0.07	0.72 ± 0.24
3	−1.30 ± 0.09	1.47 ± 0.43
4	−0.98 ± 0.03	2.15 ± 0.54
5	0.0 ± 0.1	3.08 ± 0.33
cisplatin	−2.21 ± 0.06	n.d.[c]

[a]Errors are estimated from the standard deviations of repeated experiments. [b]Errors are the standard deviations obtained from the use of seven different computational algorithms as employed by ALOGSP 2.1. [c]Not determined.

The values are displayed in Table 3. The calculated ligand log *P* values are linearly proportional to the experimentally measured complex log *P* values (Figure 2). As expected, more lipophilic ligands give rise to more lipophilic complexes.

Aquation and Anation Rates. The stabilities of **1**−**5** in water and phosphate buffered saline (PBS), pH 7.4, at 37 °C were determined by NMR spectroscopy. The compounds bearing nonfluorinated β-diketonate ligands, **1**, **3**, and **5**, exhibited no changes in their ^{1}H NMR spectra in either medium for up to 25 d. Compounds **2** and **4**, which both have a trifluoromethyl group in the ligand backbone, slowly decomposed in water and PBS. In water, the ^{1}H NMR

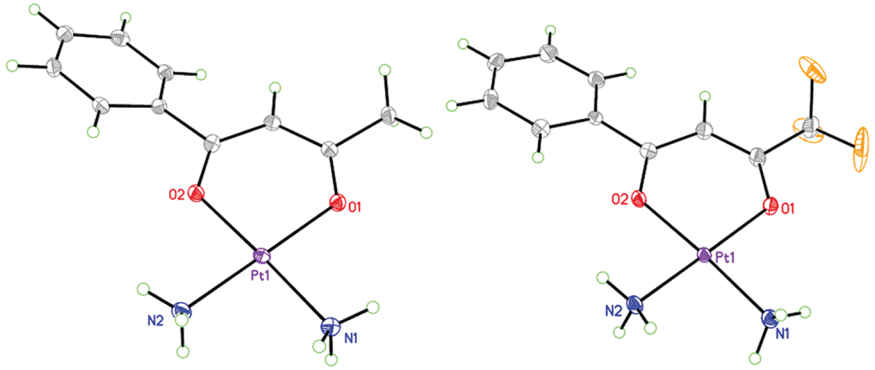

3 **4**

Figure 1. X-ray crystal structures of the complex cations of **3** (left) and **4** (right). Ellipsoids are drawn at the 50% probability level. Gray shaded ellipsoids represent carbon atoms, orange shaded ellipsoids fluorine atoms, and open green circles hydrogen atoms. The identities of the other atoms are denoted.

dx.doi.org/10.1021/jm3002857 | J. Med. Chem. 2012, 55, 5326−5336

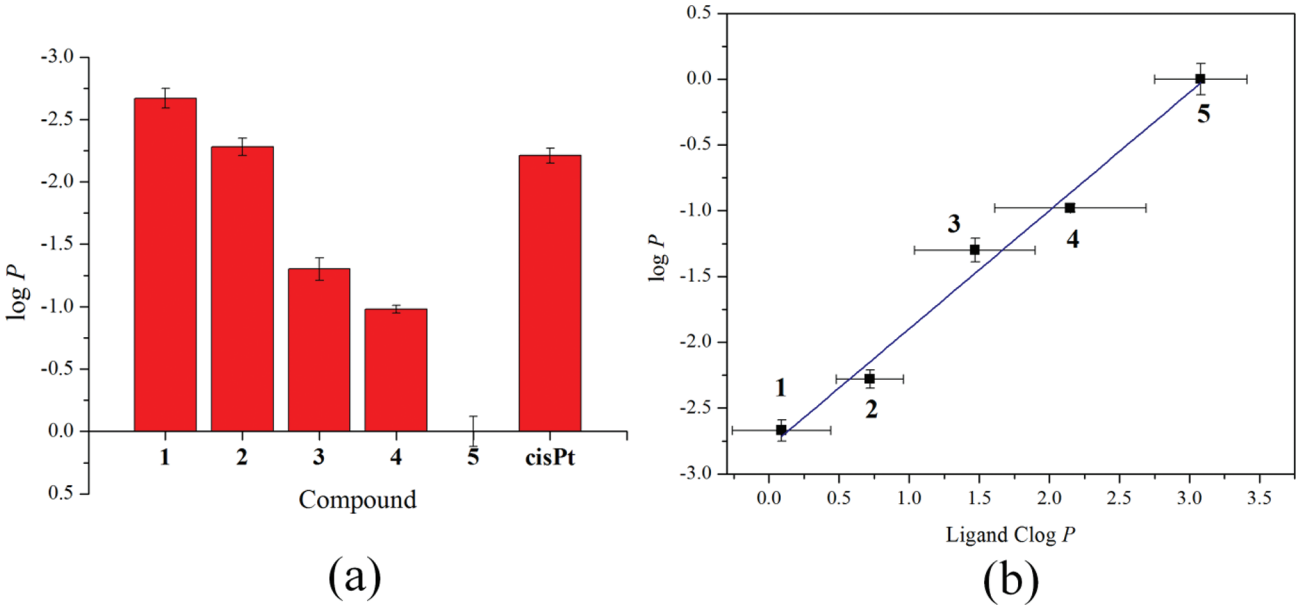

Figure 2. (a) Graphical representation of experimentally measured log *P* values of **1**–**5** and cisplatin. (b) Plot of calculated ligand log *P* (Clog *P*) values versus experimentally measured complex log *P* values. The line represents the best fit to a linear regression analysis of the data. The slope and intercept of this line are 0.90 ± 0.06 and −2.8 ± 0.1, respectively. The R^2 value is 0.98.

chemical shift at 2.00 ppm of the methyl group of **2** decayed with a half-life of 58 d and concomitant appearance of a new resonance at 2.22 ppm (Figures S17–S19, Supporting Information). Over the course of this reaction, the pH changed from 7.5 to 6.3. For **4**, the rate of decomposition was faster. The ^{19}F NMR chemical shift at −74.4 ppm of **4** disappeared with a half-life of 29 d, accompanied by the appearance of a new resonance at −76.6 ppm (Figure S20–S22, Supporting Information). The aliphatic region of the ^{1}H NMR spectrum at this final time point is marked by a sharp singlet at 2.67 ppm, which is not observed upon the initial dissolution of the complex. The pH of this solution remained at 7.5 for the duration of the experiment.

In pH 7.4 PBS, the rates of decomposition increased. The half-lives of **2** and **4** in this medium are 3.4 and 1.8 d, respectively. For **4**, the final product is the same as that observed following aquation in nonbuffered water as characterized by a ^{19}F NMR chemical shift at −76.6 ppm (Figures S23–S25, Supporting Information) and a sharp singlet in the ^{1}H NMR spectrum at 2.67 ppm. Complex **2** displays more complex reactivity in PBS. Although the major final product is the same as that observed for aquation in pure water (^{1}H δ = 2.22 ppm), two other minor products were observed by ^{1}H NMR spectroscopy having CH_3 proton resonances at 1.91 and 1.56 ppm. In addition, an intermediate with a CH_3 proton resonance at 2.25 ppm was apparent (Figures S26–S28, Supporting Information).

With the goal of characterizing the aquation and anation products of **2** and **4**, the NMR spectra of the free ligands of these complexes in PBS were investigated. Initially, the ^{1}H NMR spectrum of sodium trifluoracetylacetonate, Na(tfac), in PBS displayed a CH_3 resonance at 2.25 ppm. Upon further incubation at 37 °C for 6 d, this resonance at 2.25 ppm decayed and was replaced by a major resonance at 2.22 ppm and two minor resonances at 1.91 and 1.56 ppm. Because these signals are the same as those observed during the aquation and anation of **2**, we propose that the free tfac ligand is displaced from the platinum center as an intermediate with a chemical shift of 2.25 ppm and then undergoes ligand decomposition reactions.

For the ligand of **4**, 4,4,4-trifluorobenzoylacetone (Htfbz), two peaks in its ^{19}F NMR spectrum at −76.37 and −86.7 ppm were initially observed. These two signals possibly correspond to the keto and enol tautomers of the compound. After 6 d at 37 °C, the major species in solution is a compound characterized by a singlet in the ^{1}H NMR spectrum at 2.67 ppm and a signal in the ^{19}F NMR spectrum at −76.41 ppm. These spectroscopic signals are consistent with the major species observed after the aquation and anation of **4**. Thus, as for **2**, dissociation from the platinum center precedes ensuing hydrolytic decomposition of the fluorinated β-diketonate ligand.

Cancer Cell Cytotoxicity. The antiproliferative activities of **1**–**5** and cisplatin were determined in HeLa (human cervical cancer), A549 (human lung cancer), U2OS (human osteosarcoma), and MCF-7 (human breast cancer) cell lines by the MTT assay. The cells were treated continuously for 72 h. The resulting 50% growth inhibitory concentration (IC_{50}) values are summarized in Table 4 and graphically depicted in Figure 3. Representative dose–response curves are shown in the Supporting Information (Figures S29–S32). For the four cell lines tested, **1** is the least cytotoxic of the five complexes, with IC_{50} values ranging from 24 to 76 μM. The IC_{50} values of **3** vary between 7 and 33 μM, indicating slightly greater cytotoxicity than **1**. Complexes **2**, **4**, and **5** exhibit cytotoxicities comparable to that of cisplatin. The IC_{50} values for these compounds are generally <10 μM, except for **2** in MCF-7 cells where the IC_{50} is 15 μM.

Because **4** is on average the most cytotoxic of the five complexes, it was submitted to the NCI for evaluation in the NCI-60 tumor cell panel screen.[46] In this screen, a single-dose cytotoxicity measurement is performed in 60 cell lines with distinctive drug sensitivity profiles. This process can identify drug candidates with unique anticancer activity spectra based on which cell lines are sensitive or resistant to a compound of interest. Using the COMPARE algorithm, activity spectra can be quantitatively correlated with those of other compounds in the NCI database. Pearson correlation coefficients are used to evaluate similarities in activity spectra. Correlations coefficients close to one indicate compounds with similar mechanisms of

dx.doi.org/10.1021/jm3002857 | J. Med. Chem. 2012, 55, 5326–5336

Table 4. IC_{50} Values of 1−5 and Cisplatin in HeLa, A549, U2OS, and MCF-7 Cell Lines and Cellular Uptake in HeLa Cells

	IC_{50} (μM)[a]				
compd	HeLa	A549	U2OS	MCF-7	HeLa cellular uptake (ng Pt/10^6 cells)[b]
1	32 ± 5	28 ± 9	24 ± 2	76 ± 2	6 ± 2
2	2.9 ± 0.7	2.2 ± 0.6	4.1 ± 0.8	15 ± 2	29 ± 9
3	24 ± 4	7 ± 2	8 ± 2	33 ± 6	83 ± 8
4	3 ± 1	1.3 ± 0.2	1.6 ± 0.5	4.3 ± 0.3	160 ± 20
5	6.7 ± 0.7	1.3 ± 0.3	2.7 ± 0.7	3.1 ± 0.5	520 ± 80
cisplatin	2.1 ± 0.1	3.2 ± 0.6	5 ± 2	14 ± 3	14 ± 2

[a]Errors are standard deviations determined from at least three independent experiments. [b]The errors are determined by error propagation equations, as described in ref 63.

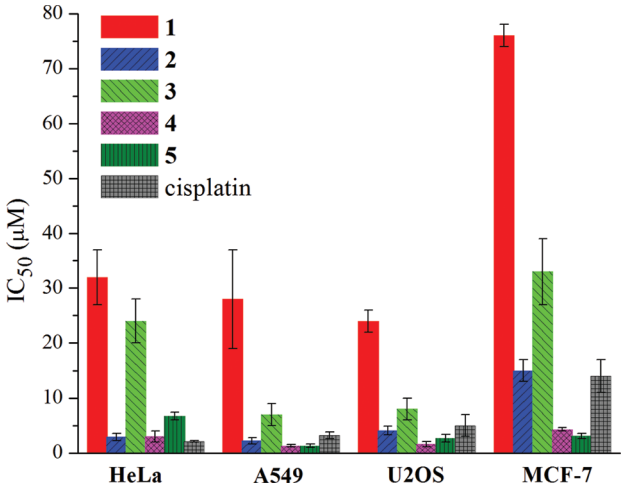

Figure 3. Graphical representation of IC_{50} values for **1**−**5** and cisplatin in HeLa, A549, U2OS, and MCF-7 cell lines.

action and resistance profiles. The average cell growth percentage of the 60 cell lines after 48 h of treatment with 10 μM **4** was 89.65% (Figure S33, Supporting Information), indicating slight growth inhibitory action. Compound **4** showed the greatest efficacy against central nervous system (CNS) cancer, where the average cell growth was 64.52%. Results of the COMPARE algorithm are summarized in Table 5.

Table 5. Results of COMPARE Analysis of 4

Compound **4** (NSC No. 761186) COMPARE Analysis				
rank	PCC[a]	NSC no.[b]	name	biological mechanism of action
1	0.589	95466	PCNU	alkylating agent
2	0.569	750	busulfan	alkylating agent
3	0.559	301739	mitoxantrone	type II topoisomerase inhibitor
4	0.534	355644	anthrapyrazole	type II topoisomerase inhibitor
5	0.506	178248	chlorozotocin	alkylating agent
6	0.501	357704	cyanomorpholino-ADR	alkylating agent
7	0.495	3088	chlorambucil	alkylating agent
8	0.491	132313	dianhydrogalactitol	alkylating agent
9	0.489	119875	cisplatin	alkylating agent
10	0.485	353451	mitozolamide	alkylating agent

[a]Pearson correlation coefficient. [b]Compound identification number utilized by the NCI.

Cellular Uptake. The uptake of cisplatin and **1**−**5** by HeLa cells after a 4 h exposure time at 10 μM concentration was measured by graphite furnace atomic absorption spectroscopy (GFAAS). The results are tabulated in Table 4. The cellular uptake correlates with the lipophilicity of the compound in an exponential fashion (Figure 4). The most lipophilic complex, **5**,

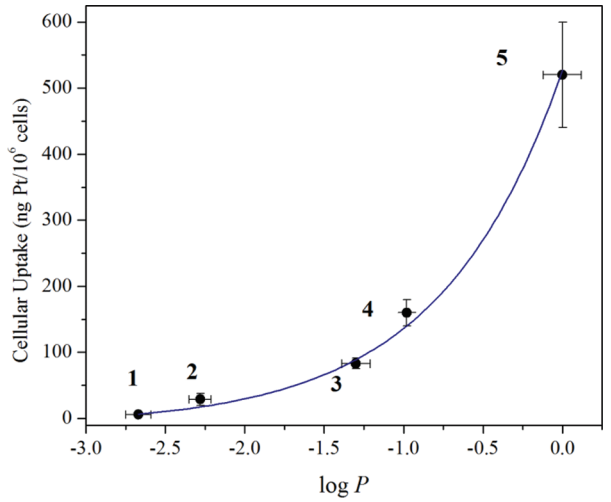

Figure 4. Plot of complex log *P* values versus cellular uptake. The blue line is an exponential fit of the data.

is taken up to the greatest extent (520 ± 80 ng Pt/10^6 cells), whereas the least lipophilic complex is taken up the least (6 ± 2 ng Pt/10^6 cells). All complexes except **1** have larger accumulation in HeLa cells than cisplatin under similar conditions.

Intracellular DNA Platination. Because platinum-based drugs exert their cytotoxic effects by the formation of DNA cross-links, the extent to which **1**−**5** bind to intracellular DNA was measured. HeLa cells were treated with 100 μM of the platinum complexes for 4 h and then incubated for an additional 16 h in platinum-free growth medium. The nuclear DNA was isolated, and the quantity of bound platinum was measured by GFAAS. The results of this study are shown in Table 6. The extent of DNA platination follows the order **5** ≈ **4** > cisplatin > **3** ≈ **2** > **1**.

DISCUSSION

The use of β-diketonate ligands as leaving groups for traditional *cis*-diammineplatinum(II) anticancer agents is relatively unexplored. Here, we investigated the physical properties and anticancer efficacy for a small set of compounds in this class. The five β-diketonate ligands chosen for this study were systematically varied, by addition of either a phenyl ring or a trifluoromethyl group (Chart 1). Such variations allowed us to monitor how alterations of the hydrophobicity and electron-withdrawing

dx.doi.org/10.1021/jm3002857 | J. Med. Chem. 2012, 55, 5326−5336

Table 6. Intracellular DNA Platination in HeLa Cells Induced by Cisplatin and 1−5[a]

compd	Pt/DNA (pmol/μg)
cisplatin	1.58 ± 0.97
1	0.063 ± 0.012
2	0.30 ± 0.07
3	0.35 ± 0.24
4	14 ± 3
5	23 ± 10

[a]Reported errors are the standard deviations from at least three experiments.

properties of the leaving group ligand translate into differences in anticancer efficacy in vitro.

The three synthetic methodologies employed to prepare **1**−**5** are outlined in Scheme 1. For **1** and **2**, the sulfate salt of the *cis*-diamminediaquaplatinum(II) cation was utilized. The treatment of this cation with $Ba(acac)_2$ or $Ba(tfac)_2$ produced **1** or **2**, each of which was subsequently isolated from the aqueous solution, and $BaSO_4$ as an insoluble white solid. For the syntheses of **3** and **4**, the nitrate salt of the *cis*-diamminediaquaplatinum(II) cation was treated with Na(bzac) or Na(tfbz). The $NaNO_3$ byproduct of the reaction was washed away using cold water with little product loss because **3** and **4** are only sparingly soluble in water. The low aqueous solubility of the ligand Hdbm necessitated the use of *N*,*N*-dimethylformamide (DMF) as the solvent. Activation of cisplatin in DMF with $AgNO_3$ followed by treatment of Na(dbm) afforded **5** after the appropriate reaction workup, albeit in lower yields. The preparation of the analogous hexafluoroacetylacetonate (hfac) complex was also attempted. None of the three synthetic methodologies described here provided access to the desired platinum-hfac complex. After reaction workup, unidentified green−blue residues were obtained. We propose that the difficulties associated with obtaining this complex may arise from the lability of the strongly electron-withdrawing hfac ligand.

Characterization data including ESI-MS, elemental analysis, IR spectroscopy, and multinuclear NMR spectroscopy are consistent with the proposed structures and elemental compositions of **1**−**5**. Of particular interest are the ^{195}Pt NMR chemical shifts of the new complexes. This parameter is very sensitive to the platinum coordination environment and can span a region of >13,000 ppm.[47−49] In the present case, the ^{195}Pt NMR chemical shifts of **1**−**5** range over 139 ppm (Table 1), indicating that peripheral substituents on the β-diketonate ligands influence the electron density at the platinum center. Complex **1** has the most shielded Pt nucleus, which resonates at −1593 ppm, whereas **4** is most deshielded with the ^{195}Pt chemical shift appearing at −1454 ppm. The chemical shift for this class of compounds appears to depend on the electron-withdrawing strength of the ligand. The trifluoromethyl substituents of **2** and **4** deshield the Pt nucleus by approximately 100 ppm relative to their analogues, **1** and **3**, which lack trifluoromethyl groups. The phenyl groups of **3**, **4**, and **5** also deshield the Pt nucleus, but to a lesser degree than the trifluoromethyl groups. Compared to their analogues having no phenyl groups, **3**, **4**, and **5** are deshielded by 20−44 ppm. The X-ray crystal structures of **3** and **4** display the expected coordination geometries (Figure 1). The complexes are structurally similar, with comparable interatomic distances and angles (Table 2). A related compound, [Pt(acac)(*trans*-1*R*,2*R*-diaminocyclohexane)](acac), has also been structurally characterized,[50] and its bond metrics resemble those of **3** and **4**.

An important physical property that affects the biodistribution of a drug candidate is its lipophilicity. The lipophilicity of a compound can be quantitatively evaluated by its log *P* values, where *P* is the water−octanol partition coefficient. More positive log *P* values correspond to more lipophilic complexes, whereas more negative log *P* values correspond to more hydrophilic ones. The log *P* values for cisplatin and **1**−**5** are given in Table 3 and Figure 2. The addition of lipophilic groups to the β-diketonate ligands increases the log *P* values of the resulting complex. Thus, the lipophilicity can be tuned with the appropriate choice of functional groups. For comparison, the log *P* values of the free ligands in their diketo forms were computed with an online program. A linear correlation exists between the calculated log *P* values of the ligands and the experimentally measured log *P* values of the complexes, as shown in Figure 2. The slope of the best-fit line is 0.90. This value, which is close to 1, indicates that coordination of the β-diketonate ligand to the *cis*-diammineplatinum(II) moiety affects its lipophilicity in an additive manner, consistent with the additive properties of substituent hydrophobicity constants.[51] The intercept of the best fit line is −2.8, which can be interpreted as the substituent hydrophobicity constant for the $\{Pt(NH_3)_2\}^+$ moiety in this class of compounds.

After establishing that different substituents on the β-diketonate ligands have a predictable and significant effect on the lipophilicities of **1**−**5**, we investigated how these substituents can modulate the reactivities of the complexes. The stabilities of **1**−**5** in water and in pH 7.4 phosphate-buffered saline at 37 °C were assessed by NMR spectroscopy. In either water or PBS, there was no sign of decomposition for **1**, **3**, and **5** for up to 25 d. Compounds **2** and **4** decomposed in water with half-lives of 58 and 29 d, respectively, and in PBS with half-lives of 3.4 and 1.8 d, respectively. The observation that the nonfluorinated complexes, **1**, **3**, and **5**, appear to have an indefinite lifetime in water and aqueous buffer indicates that the strongly electron-withdrawing properties of the trifluoromethyl groups in **2** and **4** are responsible for the increased reactivities of these complexes. In this context, however, it should be noted that **2** and **4** are still significantly more inert than cisplatin, which has an aqueous solution half-life of 2 h.[52] In PBS, which contains 137 mM NaCl and 10 mM P_i, the half-lives of **2** and **4** decrease to 3.4 and 1.8 d indicating that the high ion concentration plays a role in their reactivities. Carboplatin, which is stable for up 60 d in water,[53] has increased reactivity in the presence of high phosphate and chloride ion concentrations, the chemistry proceeding by direct anion attack on the complex and not requiring an aqua intermediate.[54] A similar process most likely explains the increased rates of decomposition of **2** and **4** in PBS relative to pure water as the solvent.

The antiproliferative activities of the complexes were assessed in four human cancer cell lines. IC_{50} values are displayed in Table 4 and graphically compared in Figure 3. The general trend of cytotoxicity among the four cell lines follows the order **1** < **3** < **2** ≈ **4** ≈ **5**. Compounds **2**, **4**, and **5** have IC_{50} values comparable to or lower than those of cisplatin. The differences in observed cytotoxicities among the five complexes can be attributed to variations in lipophilicity and reaction kinetics conferred by the β-diketonate leaving group ligands because the DNA-binding *cis*-diammineplatinum(II) fragment is the same in all five complexes as well as cisplatin.

The cellular uptake properties of the five complexes and cisplatin were measured in HeLa to see whether this parameter

dx.doi.org/10.1021/jm3002857 | J. Med. Chem. 2012, 55, 5326−5336

might be the dominant factor in determining cytotoxicity. The results are summarized in Table 4. As shown in Figure 4, the cellular uptake is a function of lipophilicity of the platinum complex. This correlation suggests that these complexes are dependent on a passive diffusion uptake mechanism. Given that these complexes are cations, they may also take advantage of organic cation transporters for selective transport into cancer cells, like oxaliplatin.[55] No correlation, however, was observed between cellular uptake and IC_{50} values for the five complexes (Figure S34, Supporting Information). This result indicates that the reaction kinetics of the complexes must also play a role in their biological activities. Consistent with this hypothesis is the observation that the fluorinated complexes, **2** and **4**, exhibit comparable or better cytotoxicities than **5** despite the fact that over twice as much **5** is taken up by cells. The increased reactivities of **2** and **4** in water and buffer are probably why they display comparable cytotoxicity to **5**, even though they are present at significantly lower concentrations within the cell. A similar correlation between aquation rates and activity is observed in a series of carboplatin derivatives bearing fluorinated CBDCA leaving group ligands.[15] There is rapid aquation of the fluorinated CBDCA relative to that of the nonfluorinated ligands, which is most likely responsible for the increased cytotoxic activity of the fluorinated derivatives relative to underivatized carboplatin.[15]

The amount of platinum found on the DNA of HeLa cells treated with cisplatin and **1**−**5** (Table 6) is not directly correlated with the IC_{50} values of the complexes, although the least active complex, **1**, does induce the least amount of DNA platination. However, for determination of the IC_{50} values the cells were treated for a continuous 72 h period, whereas for the DNA platination measurements, cells were treated at a high concentration for 4 h and then allowed to incubate for an additional 16 h in the absence of platinum. During this 16 h post-treatment period, efflux of platinum complexes out of the cell might become an important factor. Additionally, cellular targets other than DNA could modulate the cytotoxic activities of **1**−**5**. The balance between lipophilicity and reactivity in the formation of Pt-DNA adducts is still apparent, however. Complexes **2** and **3** platinate DNA to a similar extent (≈ 0.3 pmol Pt/μg DNA), as do complexes **4** and **5** (14−23 pmol Pt/μg DNA). Cellular accumulation studies indicate that **3** and **5** are taken up to a much greater extent than **2** and **4**, owing to their greater lipophilicities. The similar DNA platination levels of these complexes probably reflects the higher reactivities of the fluorinated complexes **2** and **4**, which compensates for their lower intracellular abundance.

Among the compounds studied, **4** has the optimal balance of lipophilicity and reactivity. The average IC_{50} value of this complex in the four cells lines tested is 2.6 μM, the lowest among the five complexes tested. For this reason, **4** was submitted to the National Cancer Institute for testing in the NCI-60 tumor cell panel screen. As described above, the NCI-60 tumor cell panel screen utilizes 60 different cell lines with distinct sensitivity profiles and measures the cell growth inhibitory action of a compound of interest, initially at a single dose. Differential cell growth inhibition among the 60 cell lines indicates the compound's spectrum of activity, which can be quantitatively compared to that of other compounds in the database via the COMPARE algorithm. For **4**, the average cell growth percent among the 60 cell lines after a single dose (10 μM) treatment was 89.65% relative to the complex-free control (Figure S33, Supporting Information). The apparent lower activity of **4** in the NCI-60 tumor cell screen compared to that observed in our laboratory is most likely the result of different experimental conditions.[56] The shorter incubation time (48 h), the use of RPMI as culture medium, different initial cell densities, and use of the sulforhodamine B (SRB) assay by the NCI screen are plausible reasons for the difference. In fact, higher IC_{50} values are typically measured with the SRB compared to the MTT assay because the former measures total protein content instead of mitochondrial activity.[57] The COMPARE algorithm was utilized to investigate how the spectrum of activity of **4** matches that of other anticancer agents in the NCI database. Table 5 lists the ten anticancer compounds with the highest correlation coefficients with the spectrum of activity of **4**. Eight of these ten compounds are known DNA alkylating agents. Cisplatin is one of the top ten with a Pearson correlation coefficient of 0.489. These correlations indicate that **4** and the related β-diketonato complexes act, as anticipated, by binding DNA, with the β-diketonate ligands serving as the leaving groups. The relatively high correlation with the activity of cisplatin is consistent with the formation of similar DNA cross-links. The Pearson correlation coefficient comparing the spectra of activity of cisplatin and carboplatin is 0.798[7] and is therefore much greater than that for **4** and cisplatin. The β-diketonate ligand of **4** apparently has a larger influence on the cell line selectivity than the CBDCA ligand of carboplatin. This observation may have important implications in the design of new cisplatin analogues, which differ only by the nature of their leaving group ligands.

CONCLUSIONS

This article describes the first systematic study of the physical properties and in vitro anticancer efficacy of a series of *cis*-diammineplatinum(II) complexes with β-diketonate leaving group ligands. Our results indicate that modifications of the β-diketonate ligands predictably affect both the lipophilicity and reactivity of the resulting platinum complexes. The lipophilicity of these compounds is important because it dictates the degree of cellular uptake, whereas optimal reactivity kinetics ensure that a significant amount of platinum can bind to DNA or other cellular targets within the biologically relevant time frame. Of the compounds presented here, **4** exhibited the greatest cytotoxicity on average. The trifluorobenzoylacetonate (tfbz) ligand of **4** carries both a phenyl and trifluoromethyl group. These two groups appear to provide an optimal combination of lipophilicity and reactivity for biological activity. The NCI-60 tumor cell screen revealed **4** to have a spectrum of activity similar to that of other alkylating agents, a category that often includes cisplatin. Like carboplatin, which has a similar spectrum of activity as that of cisplatin and is used as a less toxic alternative, the present β-diketonate complexes may find similar roles in future pharmaceutical applications.

EXPERIMENTAL SECTION

Materials and Methods. All synthetic procedures were performed under normal atmospheric conditions without exclusion of oxygen or moisture. Cisplatin and $Ba(acac)_2 \cdot H_2O$ were purchased from Strem Chemicals and used as received. The β-diketonate ligands were obtained from Alfa Aesar and used as received. Distilled water and analytical grade DMF were employed as solvents. The purities (>95%) of the newly synthesized compounds were verified by the absence of unidentified peaks in their ^1H NMR spectra (Figures S1−S16, Supporting Information) and by elemental analyses.

Physical Measurements. NMR measurements were recorded on a Bruker DPX-400 spectrometer in the MIT Department of Chemistry

Instrumentation Facility at 20 °C. ^{1}H and $^{13}C\{^{1}H\}$ NMR spectra were referenced internally to residual solvent peaks, and chemical shifts are expressed relative to tetramethylsilane, $SiMe_4$ (δ = 0 ppm). $^{195}Pt\{^{1}H\}$ and $^{19}F\{^{1}H\}$ NMR spectra were referenced externally using standards of K_2PtCl_4 in D_2O (δ = −1628 ppm relative to Na_2PtCl_6) and trifluorotoluene (δ = −63.72 ppm relative to $CFCl_3$), respectively. Fourier transform infrared (FTIR) spectra were recorded with a ThermoNicolet Avatar 360 spectrophotometer running the OMNIC software. Samples were prepared as KBr disks. Electrospray ionization mass spectrometry (ESI-MS) measurements were acquired on an Agilent Technologies 1100 series LC-MSD trap. Graphite furnace atomic absorption spectrometry was carried out using a Perkin-Elmer AAnalyst600 GFAAS. Elemental analyses were performed by a commercial laboratory.

Synthesis of [Pt(acac)(NH$_3$)$_2$](SO$_4$)$_{0.5}$ (1). A suspension of cisplatin (0.500 g, 1.67 mmol) and Ag_2SO_4 (0.499 g, 1.60 mmol) in 15 mL of water was stirred at room temperature in the dark for 12 h. The resulting solids were filtered to remove white AgCl, and to the filtrate, a 10 mL aqueous solution of $Ba(acac)_2{\cdot}H_2O$ (0.268 g, 0.800 mmol) was added dropwise, inducing the precipitation of insoluble $BaSO_4$. This suspension was stirred at room temperature for 3 h and then filtered. The orange−brown filtrate was concentrated to dryness under reduced pressure at 60 °C to afford a brown residue. The residue was dissolved in 5 mL of MeOH at 65 °C and filtered through Celite to remove an insoluble impurity. Treatment of this MeOH solution with 15 mL of Et_2O yielded the desired compound as a white solid, which was isolated by centrifugation and washed an additional two times with 10 mL of Et_2O before drying in vacuo. Yield: 0.438 g (70%). Mp >140 °C (gradual darkening and decomposition). ^{1}H NMR (400 MHz, MeOD-d_4): δ 5.58 (s, 1H), 1.85 (s, 6H). $^{13}C\{^{1}H\}$ NMR (100 MHz, MeOD-d_4): δ 185.6, 103.3, 26.1. $^{195}Pt\{^{1}H\}$ NMR (86 MHz, MeOD-d_4): δ −1593. IR (KBr, cm^{-1}): 3446 m, 3179 s, 3134 s, 3075 m, 1564 s, 1525 vs, 1427 w, 1382 m, 1331 w, 1304 m, 1284 w, 1194 w, 1112 vs, 1024 w, 951 w, 938 w, 869 w, 831 w, 772 vw, 659 m, 619 m, 541 w, 480 w. ESI-MS (pos. ion mode, MeOH): m/z 328.1 ([M]$^+$, calcd. 328.1). Anal. Calcd. for **1**, $C_5H_{13}N_2O_4PtS_{0.5}$: C, 15.96; H, 3.48; N, 7.44. Found: C, 15.82; H, 3.51; N, 6.94.

Synthesis of [Pt(tfac)(NH$_3$)$_2$](SO$_4$)$_{0.5}$ (2). A suspension of cisplatin (0.500 g, 1.67 mmol) and Ag_2SO_4 (0.499 g, 1.60 mmol) in 15 mL of water was stirred at room temperature in the dark for 12 h. The resulting suspension was filtered to remove white AgCl, and to the filtrate, a 10 mL hot (70 °C) aqueous solution of $Ba(OH)_2{\cdot}8H_2O$ (0.252 g, 0.800 mmol) and Htfac (0.246 g, 1.60 mmol) was added dropwise, inducing the precipitation of insoluble $BaSO_4$. The yellow suspension was stirred at room temperature for 3 h and then filtered. The bright yellow filtrate was concentrated to dryness under reduced pressure at 60 °C to afford the desired compound as a yellow solid. The yellow solid was resuspended in 5 mL of cold H_2O, filtered, and washed sequentially with 5 mL of cold H_2O and twice with 5 mL of Et_2O before being dried in vacuo. Yield: 0.314 g (44%). Mp >190 °C (gradual darkening and decomposition). ^{1}H NMR (400 MHz, MeOD-d_4): δ 6.10 (s, 1H), 2.00 (s, 3H). $^{19}F\{^{1}H\}$ NMR (376 MHz, MeOD-d_4): δ −76.43. $^{195}Pt\{^{1}H\}$ NMR (86 MHz, MeOD-d_4): δ −1497. IR (KBr, cm^{-1}): 3341 m, 3101 s, 2917 w, 1592 s, 1526 m, 1458 w, 1367 w, 1304 vs, 1240 m, 1194 m, 1138 vs, 876 w, 805 w, 743 w, 668 w, 618 m, 448 w. ESI-MS (pos. ion mode, MeOH): m/z 382.0 ([M]$^+$, calcd. 382.0). Anal. Calcd. for **2**, $C_5H_{10}F_3N_2O_4PtS_{0.5}$: C, 13.96; H, 2.34; N, 6.51. Found: C, 13.81; H, 2.48; N, 6.41.

Synthesis of [Pt(bzac)(NH$_3$)$_2$](NO$_3$) (3). A mixture of cisplatin (0.500 g, 1.67 mmol) and $AgNO_3$ (0.553 g, 3.25 mmol) in 10 mL of water was stirred in the absence of light for 12 h at room temperature. The resulting suspension was filtered to remove white AgCl, and a hot aqueous solution (70 °C, 10 mL) of Hbzac (0.264 g, 1.63 mmol) and NaOH (0.065 g, 1.6 mmol) was added dropwise to the filtrate, forming a yellow suspension, which was allowed to stir at room temperature for 4 h. The mixture was concentrated in vacuo at 60 °C to a volume of 8 mL and then filtered to collect the desired compound as a pale yellow solid. This solid was suspended in 10 mL of Et_2O and isolated by centrifugation twice to remove an ether-soluble impurity, before being dried in vacuo. Yield: 0.400 g (53%). Mp 160 °C (gradual darkening), 210−215 °C (dec). ^{1}H NMR (400 MHz, MeOD-d_4): δ 7.95 (d, 2H), 7.55 (t, 1H), 7.41 (app t, 2H), 6.31 (s, 1H), 2.00 (s, 3H). $^{13}C\{^{1}H\}$ NMR (100 MHz, MeOD-d_4): δ 187.5, 178.2, 138.0, 132.7, 129.9, 128.4, 100.3, 26.7. $^{195}Pt\{^{1}H\}$ NMR (86 MHz, MeOD-d_4): δ −1572. IR (KBr, cm^{-1}): 3435 w, 3279 s, 3200 m, 3116 m, 1599 w, 1584 m, 1548 s, 1514 vs, 1490 m, 1451 m, 1397 s, 1383 s, 1341 vs, 1312 vs, 1221 w, 957 w, 878 w, 779 m, 713 m, 689 w, 671 w, 580 vw, 483 vw. ESI-MS (pos. ion mode, MeOH): m/z 390.1 ([M]$^+$, calcd. 390.1), 842.0 ([2M+NO$_3$]$^+$, calcd. 842.1). Anal. Calcd. for **3**, $C_{10}H_{15}N_3O_5Pt$: C, 26.55; H, 3.34; N, 9.29. Found: C, 26.30; H, 3.26; N, 9.20.

Synthesis of [Pt(tfbz)(NH$_3$)$_2$](NO$_3$) (4). A mixture of cisplatin (0.500 g, 1.67 mmol) and $AgNO_3$ (0.553 g, 3.25 mmol) in 10 mL of water was stirred in the absence of light for 12 h at room temperature. The resulting suspension was filtered to remove white AgCl, and a hot aqueous solution (70 °C, 10 mL) of Htfbz (0.352 g, 1.63 mmol) and NaOH (0.065 g, 1.6 mmol) was added dropwise to the filtrate, forming a bright yellow suspension, which was allowed to stir at room temperature for 4 h. The mixture was then concentrated to dryness under reduced pressure at 60 °C to afford an orange residue. The residue was dissolved in 10 mL of acetone and filtered to remove the $NaNO_3$ byproduct. On top of the bright yellow filtrate, 10 mL of Et_2O was carefully layered, and bright yellow crystals of the desired compound formed overnight. The supernatant was decanted, and the crystals were washed with 5 mL of cold water to remove a white solid impurity, followed by 5 mL of Et_2O prior to drying in vacuo. Yield: 0.215 g (25%). Mp >230 °C (gradual darkening and decomposition). ^{1}H NMR (400 MHz, MeOD-d_4): δ 8.07 (d, 2H), 7.71 (t, 1H), 7.50 (app t, 2H), 6.72 (s, 1H). $^{13}C\{^{1}H\}$ NMR (100 MHz, MeOD-d_4): δ 184.2, 166.9 (q, $^{2}J_{CF}$ = 34 Hz), 137.0, 134.6, 130.5, 128.9, 119.3 (q, $^{1}J_{CF}$ = 282 Hz), 96.5. $^{19}F\{^{1}H\}$ NMR (376 MHz, MeOD-d_4): δ −76.17. $^{195}Pt\{^{1}H\}$ NMR (86 MHz, MeOD-d_4): δ −1454. IR (KBr, cm^{-1}): 3431 m, 3342 m, 3213 m, 1592 s, 1564 vs, 1536 s, 1490 w, 1458 w, 1420 m, 1384 s, 1326 s, 1303 vs, 1259 m, 1203 s, 1137 s, 1024 w, 948 w, 813 w, 776 m, 697 s, 619 w, 572 w. ESI-MS (pos. ion mode, MeOH): m/z 444.1 ([M]$^+$, calcd. 444.0), 950.1 ([2M+NO$_3$]$^+$, calcd. 950.1). Anal. Calcd. for **4**, $C_{10}H_{12}F_3N_3O_5Pt$: C, 23.72; H, 2.39; N, 8.30. Found: C, 23.75, H, 2.36, N, 8.41.

Synthesis of [Pt(dbm)(NH$_3$)$_2$](NO$_3$) (5). Cisplatin (750 mg, 2.50 mmol) and $AgNO_3$ (828 mg, 4.87 mmol) were stirred in 6 mL of DMF at room temperature for 12 h in the absence of light. The resulting suspension was filtered to remove AgCl. The pale yellow filtrate was added dropwise to Na_2CO_3 (321 mg, 3.00 mmol) and Hdbm (560 mg, 2.50 mmol) in 5 mL of DMF. This mixture was stirred at room temperature for 3.5 h and then filtered. The filtrate was concentrated to dryness under vacuum at 60 °C to obtain an orange oily residue. This residue was dissolved in 10 mL of MeOH and filtered. The addition of Et_2O (40 mL) afforded the desired product as a yellow solid, which was isolated by filtration, washed with cold H_2O (4 °C, 20 mL) and Et_2O (20 mL), and dried under vacuum. Yield: 0.306 g (24%). Mp 221−229 °C (dec). ^{1}H NMR (400 MHz, MeOD-d_4): δ 8.07 (d, 4H), 7.60 (t, 2H), 7.47 (t, 4H), 6.96 (s, 1H). $^{13}C\{^{1}H\}$ NMR (100 MHz, MeOD-d_4): δ 179.9, 138.5, 132.9, 130.0, 128.4, 97.5. $^{195}Pt\{^{1}H\}$ NMR (86 MHz, MeOD-d_4): δ −1528. IR (KBr, cm^{-1}): 3438 w, 3278 m, 3198 m, 3058 w, 1589 m, 1530 vs, 1487 s, 1454 m, 1385 s, 1318 s, 1237 m, 1075 w, 1024 w, 999 w, 945 w, 827 w, 757 m, 706 m, 670 m, 596 vw, 559 vw. ESI-MS (pos. ion mode, MeOH): m/z 452.0 ([M]$^+$, calcd. 452.1), 965.8 ([2M+NO$_3$]$^+$, calcd. 966.2). Anal. Calcd. for **5**·H_2O, $C_{15}H_{19}N_3O_6Pt$: C, 33.84; H, 3.60; N, 7.89. Found: C, 34.17; H, 3.24; N, 7.99.

X-ray Crystallography. Vapor diffusion of diethyl ether into methanol solutions afforded single crystal of **3** and **4**. The single crystals were mounted in Paratone oil on a cryoloop and frozen under a 110 or 100 K KRYO-FLEX nitrogen cold stream. Data were collected on a Bruker APEX CCD X-ray diffractometer with graphite-monochromated Mo−Kα radiation (λ = 0.71073 Å) controlled by the APEX2 software package.[58] Absorption corrections were applied using SADABS.[59] The structures were solved using direct methods and refined on F^2 with the SHELXTL-97 software package.[60,61] Structures

were checked for higher symmetry using PLATON.[62] All non-hydrogen atoms were located and refined anisotropically. Hydrogen atoms were placed in idealized locations and given isotropic thermal parameters equivalent to either 1.5 (terminal CH_3 or NH_3 hydrogen atoms) or 1.2 times the thermal parameter of the atom to which they were attached. Crystallographic data collection and refinement parameters (Table S1, Supporting Information) and cif files can be found in the Supporting Information. The cif files of **3** and **4** have also been deposited in the Cambridge Crystallographic Data Centre (http://www.ccdc.cam.ac.uk/) under the accession numbers CCDC 868860 and 868861, respectively.

Solution Stability Measurements. The platinum complexes were dissolved in water or pH 7.4 PBS containing 10% D_2O to a concentration of ~1 mM. The solutions were transferred to NMR tubes and incubated in a 37 °C water bath. ^1H and ^{19}F NMR spectra were obtained at various type points during the incubation. A small amount of 1,4-dioxane (δ = 3.75 ppm) was included in the samples as an internal standard for referencing ^1H NMR spectra and a sealed capillary containing aqueous KF (δ = −120.46 ppm) was used for referencing ^{19}F NMR spectra. The methyl group of **2** in the ^1H NMR spectra was integrated relative to the 1,4-dioxane reference at different time points and used for kinetic analyses. The trifluoromethyl group of **4** in the ^{19}F NMR spectra was integrated relative to the KF standard at different time points and used for kinetic analyses. Under the assumption of first-order kinetics, approximate half-lives were determined by fitting a line to a plot of ln[Pt] versus time and using the integrated first-order rate law, $\ln[Pt] = -kt + [Pt]_o$ and the relationship, $t_{1/2} = \ln 2/k$, where $[Pt]_o$ is the starting concentration of complex, k is the pseudo-first-order rate constant, t is time, and $t_{1/2}$ is the half-life. Water suppression for ^1H NMR spectra was accomplished with presaturation. The pH of the solutions was measured at the beginning and end of the desired incubation time using a DG-111-SG glass electrode calibrated with standard buffers.

Partition Coefficient Measurements. Water or PBS were stirred with octanol for 24 h and then centrifuged for 5 min to obtain octanol-saturated water and water-saturated octanol. The platinum complexes were dissolved in the octanol-saturated water, or PBS for cisplatin, to a typical concentration of 0.03 to 3 mM and then mixed with water-saturated octanol in volumetric ratios of 1:1, 1:2, and 2:1 in duplicate. The mixtures were vortexed for 0.5 h and then centrifuged for 5 min. The layers were separated carefully using a fine-gauge needle and then analyzed for Pt content by GFAAS. The partition coefficient was taken as a ratio of the concentration of platinum in the octanol layer to that in the aqueous layer ($P = c_{oct}/c_{water}$). The reported error is the standard deviation of the six measurements obtained from this protocol.

Calculated ligand log P values were obtained from the online program ALOGPS 2.1[43] available at the Virtual Computational Chemistry Laboratory.[44,45] Only the keto tautomeric form of the protonated ligand was used for these calculations. In addition to using the ALOGPS algorithm, this program also calculates log P values using several other algorithms for comparison. The values presented here are the average log P values computed for all the algorithms, and the errors reported are the standard deviation of these values.

Cell Lines and Culture Conditions. HeLa (human cervical cancer), A549 (human lung cancer), U2OS (osteosarcoma), and MCF-7 (human breast cancer) cells were grown as adherent monolayers in growth medium consisting of Dulbecco's Modified Eagle's Medium (DMEM) supplemented with 10% fetal bovine serum (FBS) and 1% penicillin/streptomycin. The cultures were grown in 25 cm^2 flasks in an incubator at 37 °C with a humidified atmosphere composed of 5% CO_2.

Cytotoxicity Assays. The colorimetric MTT assay was used to determine the cytotoxicity of cisplatin and the β-diketonate platinum complexes. Trypsinized cells were seeded into a 96-well plate at a cell density of 2000 cells/well in 200 μL of growth medium and incubated for 24 h. The medium was then removed, and 200 μL of new growth medium containing various concentrations of the platinum complexes was added. After 72 h, the medium was removed, 200 μL of a 0.8 mg/mL solution of MTT in DMEM was added, and the plate was incubated further for 4 h. The DMEM/MTT mixture was aspirated, and 200 μL of DMSO with 10% pH 10.5 glycine buffer was added to dissolve the resulting purple formazan crystals. The absorbance of the plates was read at 555 nm. Absorbance values were normalized to the platinum-free control wells and plotted as [Pt] versus % viability. IC_{50} values were interpolated from the resulting curves. The reported IC_{50} values are the averages from at least three independent experiments, each of which consisted of six replicates per concentration level. Dilutions of the platinum complexes in growth medium were made from concentrated (1−3 mM) solutions in distilled water for β-diketonate platinum complexes or pH 7.4 PBS for cisplatin.

Compound **4** was submitted to the NCI in July, 2011 for single-dose testing in the NCI-60 tumor cell screen. These tests were carried out by the NCI using their established protocols.[56]

Cellular Uptake Studies. The total platinum uptake per cell was determined using slight modifications of a previously described protocol.[63] In two 6-well plates, 3×10^5 HeLa cells per well were seeded in 3 wells with 2.5 mL of growth medium. In one of the plates, the additional 3 wells were filled with 2.5 mL of growth medium to act as blanks for nonspecific platinum adsorption on the surface of the well. After incubating for 48 h, each well in the plate containing both cells and cell-free medium was treated with 0.278 mL of a 100 μM solution of the desired compound to give an exposure concentration of 10 μM. The cells and cell-free blanks were incubated with the Pt complex for 4 h. Meanwhile, the cells in the other plate were counted with trypan blue after detachment with trypsin in order to obtain the number of cells per well. After the 4 h incubation period, the growth medium was aspirated, and all six wells were washed twice with 3 mL of pH 7.4 PBS and then treated with exactly 0.5 mL of hot (≈ 90 °C) concentrated nitric acid for 2 h. This solution was analyzed by GFAAS to determine the total Pt content per well. The amount of Pt per cell was calculated by subtracting the average amount of Pt found in the blank wells from the average amount of Pt found in the cell-containing wells and normalizing to the average number of cells per well.

Intracellular DNA Platination Measurements. Five million HeLa cells were seeded in a 100 mm Petri dish containing 9 mL of growth medium. On the following day, the cells were treated with the platinum complex at 100 μM concentration for 4 h. The growth medium was then replaced with platinum-free medium, and the cells were incubated for an additional 16 h. Cells, both floating and attached, were collected and combined. Trypsin (2 mL) was used to detach the cells. The combined cells were centrifuged for 5 min at 4 °C, and the resulting cell pellet was washed twice with 3 mL of ice-cold PBS. DNAzol (1 mL, genomic DNA isolation reagent, MRC), containing 100 μg/mL RNase A, was used to lyse the cell pellet. DNA was precipitated with 0.5 mL of absolute ethanol, washed 2 times with 75% ethanol (0.75 mL), and redissolved in 200 μL of 8 mM NaOH. The DNA concentration was determined by UV−visible spectroscopy, and platinum was quantified by GFAAS. The reported values are the average of at least three independent experiments with the error reported as the standard deviation.

■ ASSOCIATED CONTENT

Ⓢ Supporting Information

X-ray crystallographic data in CIF format, crystallographic data and refinement parameters for **3** and **4** (Table S1), multinuclear NMR spectra of **1**−**5** (Figures S1−S16), stability measurements of **2** and **4** in water and buffer (Figures S17−S28), representative dose−response curves cytotoxicity measurements (Figures S29−S32), NCI-60 tumor cell panel screen for **4** (Figure S33), and plot of cellular uptake versus IC_{50} in HeLa cells (Figure S34). This material is available free of charge via the Internet at http://pubs.acs.org.

■ AUTHOR INFORMATION

Corresponding Author

*Phone: (617)253-1892. E-mail: lippard@mit.edu.

Notes

The authors declare the following competing financial interest: S.J.L. declares a financial interest in Blend Therapeutics.

■ ACKNOWLEDGMENTS

This work was supported by the National Cancer Institute under grant CA034992. Spectroscopic instrumentation at the MIT DCIF is maintained with funding from NIH Grant 1S10RR13886-01.

■ ABBREVIATIONS USED

acac, acetylacetonate; bzac, benzoylacetonate; CBDCA, 1,1-cyclobutanedicarboxylate; cisplatin, *cis*-diamminedichloroplatinum(II); dbm, dibenzoylmethide; GFAAS, graphite furnace atomic absorption spectroscopy; hfac, hexafluoroacetylacetonate; IC_{50}, 50% growth inhibitory concentration; MTT, (3-(4,5-dimethylthiazol-2-yl)-2,5-diphenyltetrazolium bromide; DMF, *N*,*N*-dimethylformamide; PBS, phosphate buffered saline; SRB, sulforhodamine B; tfac, 1,1,1-trifluoroacetylacetonate; tfbz, 4,4,4-trifluorobenzoylacetonate; TMS, tetramethylsilane

■ REFERENCES

(1) Kelland, L. The resurgence of platinum-based cancer chemotherapy. *Nat. Rev. Cancer* **2007**, *7*, 573−584.
(2) Cvitkovic, E. Cumulative toxicities from cisplatin therapy and current cytoprotective measures. *Cancer Treat. Rev.* **1998**, *24*, 265−281.
(3) Boulikas, T.; Vougiouka, M. Cisplatin and platinum drugs at the molecular level. *Oncol. Rep.* **2003**, *10*, 1663−1682.
(4) Jamieson, E. R.; Lippard, S. J. Structure, recognition, and processing of cisplatin-DNA adducts. *Chem. Rev.* **1999**, *99*, 2467−2498.
(5) Todd, R. C.; Lippard, S. J. Inhibition of transcription by platinum antitumor compounds. *Metallomics* **2009**, *1*, 280−291.
(6) Knox, R. J.; Friedlos, F.; Lydall, D. A.; Roberts, J. J. Mechanism of cytotoxicity of anticancer platinum drugs: Evidence that *cis*-diamminedichloroplatinum(II) and *cis*-diammine-(1,1-cyclobutanedicarboxylato)platinum(II) differ only in the kinetics of their interaction with DNA. *Cancer Res.* **1986**, *46*, 1972−1979.
(7) Rixe, O.; Ortuzar, W.; Alvarez, M.; Parker, R.; Reed, E.; Paull, K.; Fojo, T. Oxaliplatin, tetraplatin, cisplatin, and carboplatin: Spectrum of activity in drug-resistant cell lines and in the cell lines of the National Cancer Institute's anticancer drug screen panel. *Biochem. Pharmacol.* **1996**, *52*, 1855−1865.
(8) van der Vijgh, W. J. F. Clinical pharmacokinetics of carboplatin. *Clin. Pharmacokinet.* **1991**, *21*, 242−261.
(9) Hollis, L. S.; Miller, A. V.; Amundsen, A. R.; Schurig, J. E.; Stern, E. W. *cis*-Diamineplatinum(II) complexes containing phosphono carboxylate ligands as antitumor agents. *J. Med. Chem.* **1990**, *33*, 105−111.
(10) Pasini, A.; D'Alfonso, G.; Manzotti, C.; Moret, M.; Spinelli, S.; Valsecchi, M. Cytotoxic diamine-platinum(II) complexes with methylsulfinyl carboxylates as the leaving groups. Synthesis, characterization, and reactivity toward chloride ions, 5′-GMP, and 9-methylguanine. *Inorg. Chem.* **1994**, *33*, 4140−4148.
(11) Zou, J.; Dou, P. Y.; Wang, K. Synthesis, antitumor activity and acute toxicity of diammine/diaminocyclohexane platinum(II) complexes with oxygen-ligating leaving group. *J. Inorg. Biochem.* **1997**, *65*, 145−149.
(12) Ho, Y.-P.; To, K. K. W.; Au-Yeung, S. C. F.; Wang, X.; Lin, G.; Han, X. Potential new antitumor agents from an innovative combination of demethylcantharidin, a modified traditional Chinese medicine, with a platinum moiety. *J. Med. Chem.* **2001**, *44*, 2065−2068.
(13) Aronov, O.; Horowitz, A. T.; Gabizon, A.; Gibson, D. Folate-targeted PEG as a potential carrier for carboplatin analogs. Synthesis and in vitro studies. *Bioconjugate Chem.* **2003**, *14*, 563−574.
(14) Aronov, O.; Horowitz, A. T.; Gabizon, A.; Fuertes, M. A.; Pérez, J. M.; Gibson, D. Nuclear localization signal-targeted poly(ethylene glycol) conjugates as potential carriers and nuclear localizing agents for carboplatin analogues. *Bioconjugate Chem.* **2004**, *15*, 814−823.
(15) Bernhardt, G.; Brunner, H.; Gruber, N.; Lottner, C.; Pushpan, S. K.; Tsuno, T.; Zabel, M. Carboplatin derivatives with superior antitumor activity compared to the parent compound. *Inorg. Chim. Acta* **2004**, *357*, 4452−4466.
(16) Brunner, H.; Gruber, N. Carboplatin-containing porphyrin−platinum complexes as cytotoxic and phototoxic antitumor agents. *Inorg. Chim. Acta* **2004**, *357*, 4423−4451.
(17) Warnecke, A.; Fichtner, I.; Garmann, D.; Jaehde, U.; Kratz, F. Synthesis and biological activity of water-soluble maleimide derivatives of the anticancer drug carboplatin designed as albumin-binding prodrugs. *Bioconjugate Chem.* **2004**, *15*, 1349−1359.
(18) Mishur, R. J.; Zheng, C.; Gilbert, T. M.; Bose, R. N. Synthesis, X-ray crystallographic, and NMR characterizations of platinum(II) and platinum(IV) pyrophosphato complexes. *Inorg. Chem.* **2008**, *47*, 7972−7982.
(19) Xie, M.; Liu, W.; Lou, L.; Chen, X.; Ye, Q.; Yu, Y.; Chang, Q.; Hou, S. Unusual dimeric chemical structure for a carboplatin analogue as a potential anticancer complex. *Inorg. Chem.* **2010**, *49*, 5792−5794.
(20) Liu, W.; Chen, X.; Ye, Q.; Xu, Y.; Xie, C.; Xie, M.; Chang, Q.; Lou, L. A novel water-soluble heptaplatin analogue with improved antitumor activity and reduced toxicity. *Inorg. Chem.* **2011**, *50*, 5324−5326.
(21) Sun, Y.; Gou, S.; Yin, R.; Jiang, P. Synthesis, antiproliferative activity and DNA binding study of mixed ammine/cyclohexylamine platinum(II) complexes with 1-(substituted benzyl) azetidine-3, 3-dicarboxylates. *Eur. J. Med. Chem.* **2011**, *46*, 5146−5153.
(22) Yin, R.; Gou, S.; Liu, X.; Lou, L. Antitumor activities and interaction with DNA of oxaliplatin-type platinum complexes with linear or branched alkoxyacetates as leaving groups. *J. Inorg. Biochem.* **2011**, *105*, 1095−1101.
(23) Bierbach, U.; Qu, Y.; Hambley, T. W.; Peroutka, J.; Nguyen, H. L.; Doedee, M.; Farrell, N. Synthesis, structure, biological activity, and DNA binding of platinum(II) complexes of the type *trans*-$[PtCl_2(NH_3)L]$ (L = planar nitrogen base). Effect of L and cis/trans isomerism on sequence specificity and unwinding properties observed in globally platinated DNA. *Inorg. Chem.* **1999**, *38*, 3535−3542.
(24) Ma, E. S. F.; Bates, W. D.; Edmunds, A.; Kelland, L. R.; Fojo, T.; Farrell, N. Enhancement of aqueous solubility and stability employing a trans acetate axis in trans planar amine platinum compounds while maintaining the biological profile. *J. Med. Chem.* **2005**, *48*, 5651−5654.
(25) Quiroga, A. G.; Pérez, J. M.; Alonso, C.; Navarro-Ranninger, C.; Farrell, N. Novel transplatinum(II) complexes with $[N_2O_2]$ donor sets. Cellular pharmacology and apoptosis induction in Pam 212-*ras* cells. *J. Med. Chem.* **2005**, *49*, 224−231.
(26) Bulluss, G. H.; Knott, K. M.; Ma, E. S. F.; Aris, S. M.; Alvarado, E.; Farrell, N. *trans*-Platinum planar amine compounds with $[N_2O_2]$ ligand donor sets: Effects of carboxylate leaving groups and steric hindrance on chemical and biological properties. *Inorg. Chem.* **2006**, *45*, 5733−5735.
(27) Aris, S. M.; Knott, K. M.; Yang, X.; Gewirtz, D. A.; Farrell, N. P. Modulation of transplanaramine platinum complex reactivity by systematic modification of carrier and leaving groups. *Inorg. Chim. Acta* **2009**, *362*, 929−934.
(28) Benedetti, B. T.; Quintal, S.; Farrell, N. P. Modulation of drug activation profiles through carboxylate ligand modification in cytotoxic *trans*-platinum planar amine compounds. *Dalton Trans.* **2011**, *40*, 10983−10988.
(29) Bischoff, H.; Berger, M. R.; Keppler, B. K.; Schmähl, D. Efficacy of *β*-diketonato complexes of titanium, zirconium, and hafnium against chemically induced autochthonous colonic tumors in rats. *J. Cancer Res. Clin. Oncol.* **1987**, *113*, 446−450.

(30) Schilling, T.; Keppler, K. B.; Heim, M. E.; Niebch, G.; Dietzfelbinger, H.; Rastetter, J.; Hanauske, A.-R. Clinical phase I and pharmacokinetic trial of the new titanium complex budotitane. *Invest. New Drugs* **1995**, *13*, 327−332.
(31) Wu, A.; Kennedy, D. C.; Patrick, B. O.; James, B. R. Ruthenium(II) acetylacetonato−sulfoxide complexes. *Inorg. Chem. Commun.* **2003**, *6*, 996−1000.
(32) Fernández, R.; Melchart, M.; Habtemariam, A.; Parsons, S.; Sadler, P. J. Use of chelating ligands to tune the reactive site of half-sandwich ruthenium(II)−arene anticancer complexes. *Chem.—Eur. J.* **2004**, *10*, 5173−5179.
(33) Melchart, M.; Habtemariam, A.; Parsons, S.; Sadler, P. J. Chlorido-, aqua-, 9-ethylguanine- and 9-ethyladenine-adducts of cytotoxic ruthenium arene complexes containing O,O-chelating ligands. *J. Inorg. Biochem.* **2007**, *101*, 1903−1912.
(34) Vock, C. A.; Renfrew, A. K.; Scopelliti, R.; Juillerat-Jeanneret, L.; Dyson, P. J. Influence of the diketonato ligand on the cytotoxicities of $[Ru(\eta^6\text{-}p\text{-cymene})(R_2acac)(PTA)]^+$ complexes (PTA = 1,3,5-triaza-7-phosphaadamantane). *Eur. J. Inorg. Chem.* **2008**, 1661−1671.
(35) Schwartz, P.; Meischen, S. J.; Gale, G. R.; Atkins, L. M.; Smith, A. B.; Walker, E. M., Jr. Preparation and antitumor evaluation of water-soluble derivatives of dichloro(1,2-diaminocyclohexane)platinum(II). *Cancer Treat. Rep.* **1977**, *61*, 1519−1525.
(36) Cleare, M. J.; Hoeschele, J. D. Anti-tumour platinum compounds. Relationship between structure and activity. *Platinum Metals Rev.* **1973**, *17*, 2−13.
(37) Muscella, A.; Calabriso, N.; Fanizzi, F. P.; De Pascali, S. A.; Urso, L.; Ciccarese, A.; Migoni, D.; Marsigliante, S. [Pt(*O*,*O*′-acac)(γ-acac)(DMS)], a new Pt compound exerting fast cytotoxicity in MCF-7 breast cancer cells via the mitochondrial apoptotic pathway. *Br. J. Pharmacol.* **2008**, *153*, 34−49.
(38) Muscella, A.; Calabriso, N.; Vetrugno, C.; Urso, L.; Fanizzi, F. P.; De Pascali, S. A.; Marsigliante, S. Sublethal concentrations of the platinum(II) complex [Pt(*O*,*O*′-acac)(γ-acac)(DMS)] alter the motility and induce anoikis in MCF-7 cells. *Br. J. Pharmacol.* **2010**, *160*, 1362−1377.
(39) Muscella, A.; Calabriso, N.; Vetrugno, C.; Fanizzi, F. P.; De Pascali, S. A.; Storelli, C.; Marsigliante, S. The platinum(II) complex [Pt(O,O′-acac)(γ-acac)(DMS)] alters the intracellular calcium homeostasis in MCF-7 breast cancer cells. *Biochem. Pharmacol.* **2011**, *81*, 91−103.
(40) Muscella, A.; Calabriso, N.; Vetrugno, C.; Fanizzi, F. P.; De Pascali, S. A.; Marsigliante, S. The signalling axis mediating neuronal apoptosis in response to [Pt(O,O′-acac)(γ-acac)(DMS)]. *Biochem. Pharmacol.* **2011**, *81*, 1271−1285.
(41) Behnke, G. T.; Nakamoto, K. Infrared spectra and structure of acetylacetonato platinum(II) complexes. I. Infrared spectra and normal coordinate analysis of potassium dichloro(acetylacetonato)platinate-(II). *Inorg. Chem.* **1967**, *6*, 433−440.
(42) Westendorf, A. F.; Zerzankova, L.; Salassa, L.; Sadler, P. J.; Brabec, V.; Bednarski, P. J. Influence of pyridine versus piperidine ligands on the chemical, DNA binding and cytotoxic properties of light activated *trans,trans,trans*-$[Pt(N_3)_2(OH)_2(NH_3)(L)]$. *J. Inorg. Biochem.* **2011**, *105*, 652−662.
(43) Tetko, I. V.; Tanchuk, V. Y. Application of associative neural networks for prediction of lipophilicity in ALOGPS 2.1 program. *J. Chem. Inf. Comput. Sci.* **2002**, *42*, 1136−1145.
(44) VCCLAB, Virtual Computational Chemistry Laboratory. http://www.vcclab.org (accessed October 2011).
(45) Tetko, I. V.; Gasteiger, J.; Todeschini, R.; Mauri, A.; Livingstone, D.; Ertl, P.; Palyulin, V. A.; Radchenko, E. V.; Zefirov, N. S.; Makarenko, A. S.; Tanchuk, V. Y.; Prokopenko, V. V. Virtual computational chemistry laboratory − design and description. *J. Comput.-Aided Mol. Des.* **2005**, *19*, 453−463.
(46) Shoemaker, R. H. The NCI60 human tumour cell line anticancer drug screen. *Nat. Rev. Cancer* **2006**, *6*, 813−823.
(47) Pregosin, P. S. Platinum-195 nuclear magnetic resonance. *Coord. Chem. Rev.* **1982**, *44*, 247−291.
(48) Priqueler, J. R. L.; Butler, I. S.; Rochon, F. D. An overview of ^{195}Pt nuclear magnetic resonance spectroscopy. *Appl. Spectrosc. Rev.* **2006**, *41*, 185−226.
(49) Still, B. M.; Kumar, P. G. A.; Aldrich-Wright, J. R.; Price, W. S. ^{195}Pt NMR - theory and application. *Chem. Soc. Rev.* **2007**, *36*, 665−686.
(50) Yuge, H.; Miyamoto, T. K. Dual behaviour of acetylacetonate anions in the hydrogen-bonded supramolecular structure (acetylacetonato-*O*,*O*′)[*trans*-(1*R*,2*R*)-diaminocyclohexane-*N*,*N*′]platinum(II) acetylacetonate. *Acta Crystallogr., Sect. C* **1997**, *53*, 1816−1819.
(51) Leo, A.; Hansch, C.; Elkins, D. Partition coefficients and their uses. *Chem. Rev.* **1971**, *71*, 525−616.
(52) Bancroft, D. P.; Lepre, C. A.; Lippard, S. J. ^{195}Pt NMR kinetic and mechanistic studies of *cis*- and *trans*-diamminedichloroplatinum-(II) binding to DNA. *J. Am. Chem. Soc.* **1990**, *112*, 6860−6871.
(53) Canovese, L.; Cattalini, L.; Chessa, G.; Tobe, M. L. Kinetics of the displacement of cyclobutane-1,1-dicarboxylate from diammine-(cyclobutane-1,1-dicarboxylato)platinum(II) in aqueous solution. *J. Chem. Soc., Dalton Trans.* **1988**, 2135−2140.
(54) Frey, U.; Ranford, J. D.; Sadler, P. J. Ring-opening reactions of the anticancer drug carboplatin: NMR characterization of *cis*-$[Pt(NH_3)_2(CBDCA\text{-}O)(5'\text{-GMP-}N7)]$ in solution. *Inorg. Chem.* **1993**, *32*, 1333−1340.
(55) Zhang, S.; Lovejoy, K. S.; Shima, J. E.; Lagpacan, L. L.; Shu, Y.; Lapuk, A.; Chen, Y.; Komori, T.; Gray, J. W.; Chen, X.; Lippard, S. J.; Giacomini, K. M. Organic cation transporters are determinants of oxaliplatin cytotoxicity. *Cancer Res.* **2006**, *66*, 8847−8857.
(56) Screening Services, NCI-60 DTP Human Tumor Cell Line Screen. http://dtp.nci.nih.gov/branches/btb/ivclsp.html (accessed Nov, 2011).
(57) Perez, R. P.; Godwin, A. K.; Handel, L. M.; Hamilton, T. C. A comparison of clonogenic, microtetrazolium and sulforhodamine B assays for determination of cisplatin cytotoxicity in human ovarian carcinoma cell lines. *Eur. J. Cancer* **1993**, *29*, 395−399.
(58) *APEX2, 2008−4.0*; Bruker AXS, Inc.: Madison, WI, 2008.
(59) Sheldrick, G. M. *SADABS: Area-Detector Absorption Correction*, University of Göttingen: Göttingen, Germany, 2008.
(60) Sheldrick, G. M. *SHELXTL-97*, 6.14; University of Göttingen: Göttingen, Germany, 2000.
(61) Sheldrick, G. M. A short history of *SHELX*. *Acta Crystallogr., Sect. A* **2008**, *64*, 112−122.
(62) Spek, A. L. *PLATON, A Multipurpose Crystallographic Tool, 91110*; Utrecht University: Utrecht, The Netherlands, 2008.
(63) Egger, A. E.; Rappel, C.; Jakupec, M. A.; Hartinger, C. G.; Heffeter, P.; Keppler, B. K. Development of an experimental protocol for uptake studies of metal compounds in adherent tumor cells. *J. Anal. At. Spectrom.* **2009**, *24*, 51−61.